

# Photodiodes and Junction Field-Effect Transistors with High UV Sensitivity

WALDEMAR VON MUENCH, CORD GESSERT, AND MAX E. KOENIGER

**Abstract**—Silicon photodiodes and photo-FET's with high blue and UV sensitivity have been produced by a special boron diffusion process. Diodes with a junction depth around  $0.2\ \mu\text{m}$  exhibit a responsivity of  $0.1\ \text{A/W}$  at  $253\ \text{nm}$ ; the maximum responsivity (with a quantum efficiency close to 100 percent) is reached at  $440\ \text{nm}$ . The responsivity of the photo-FET's operating in the photoconductive mode ( $V_{GS} = 0$ ) exceeds  $10^3\ \text{A/W}$  at  $350\ \text{nm}$ . The spectral response curve and the large-signal behavior of the photo-FET's are strongly dependent on the operating conditions.

## I. INTRODUCTION

THE SPECTRAL response of conventional silicon photodiodes (solar cells) extends from  $400$  to  $1100\ \text{nm}$ , approximately, and peaks around  $900\ \text{nm}$ . Large research and development efforts have been devoted to the improvement of silicon solar cells in the short-wavelength region of the solar spectrum ("blue-enhanced cells" and "violet cells"). This improvement was achieved mainly by a reduction of the junction depth (in the order of  $1000\ \text{\AA}$ ), whereas the impurity surface concentration was kept high ( $>10^{20}\ \text{cm}^{-3}$ ) in order to minimize the series resistance [1]. The feasibility of solar energy conversion at short wavelengths by Schottky-barrier and induced-junction cells has been investigated by several authors [2], [3]. Most work in the radiation-detector field, on the other hand, has been directed towards improving those properties which are most important for optical communication systems in the  $800$ – $1000$ -nm wavelength region. Infrared-sensing MOS-FET's employing impurity photoionization have been manufactured recently for special imaging purposes [4], [5]. There are, however, some applications (e.g., in medicine and space technology) requiring good sensitivity below  $400\ \text{nm}$ .

The low responsivity of silicon photodiodes at the short-wavelength end of the visible spectrum is due to the fact that high-energy photons are absorbed within a very shallow layer near the surface. Most of the carriers generated in this manner are lost by surface recombination. Additional losses may arise from recombination at defect centers introduced during the high-concentration donor (or acceptor) diffusion processes. The reflection coefficient of silicon is quite high in the  $200$ - to  $350$ -nm region (Fig. 1).

A conventional approach to the fabrication of UV-sensitive photodiodes is based on carrier separation within the

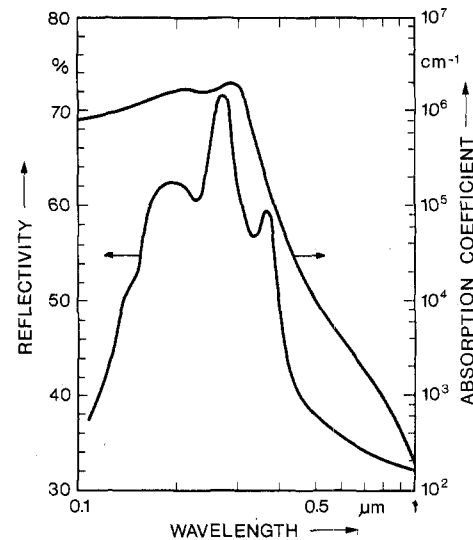


Fig. 1. Reflectivity and absorption coefficient of silicon (adapted from Grove [6]).

space-charge region of a transparent Schottky contact on n-type silicon. It is the purpose of this contribution to show that a special diffusion process with low acceptor surface concentration yields photodiodes whose UV response is superior to that of commercial Schottky-barrier detectors. The UV-sensitive region, the guard ring, and additional conductive paths (if required) are generated simultaneously. This technique can be extended to produce photoconductors and field-effect transistors with high UV sensitivity.

## II. DESIGN AND TECHNOLOGY OF UV-SENSITIVE PHOTODIODES

As seen from Fig. 1, the absorption coefficient for UV radiation ( $\lambda < 350\ \text{nm}$ ) in silicon exceeds  $10^5\ \text{cm}^{-1}$ . Consequently, electron-hole pairs are generated within a shallow ( $< 0.1\ \mu\text{m}$ ) layer close to the surface. For efficient carrier separation it is desirable to have a p-n junction whose (zero voltage) space charge extends to a plane situated at a very short distance from the surface. In addition, it is necessary to avoid impurity-induced recombination within the top (diffused) layer. Both requirements have led to the development of a diffusion process which reproducibly yields a low boron surface concentration [7]. The junction depth should be  $0.4\ \mu\text{m}$ , or less. Assuming a net surface acceptor concentration of  $4 \times 10^{16}\ \text{cm}^{-3}$ , a (p-side) space-charge layer of  $0.2\text{-}\mu\text{m}$  thickness is obtained. Thus the neutral region of the p-layer will be restricted to a distance of not more than  $0.2\ \mu\text{m}$  from the surface.

Manuscript received February 18, 1976; revised May 17, 1976.

W. von Muench and C. Gessert are with the Institut A fuer Werkstoffkunde der Technischen Universitaet Hannover, 3 Hannover, Appelstrasse 24A, Germany.

M. E. Koeniger is with Messerschmitt Boelkow Blohm Company, Ottobrunn, Germany.

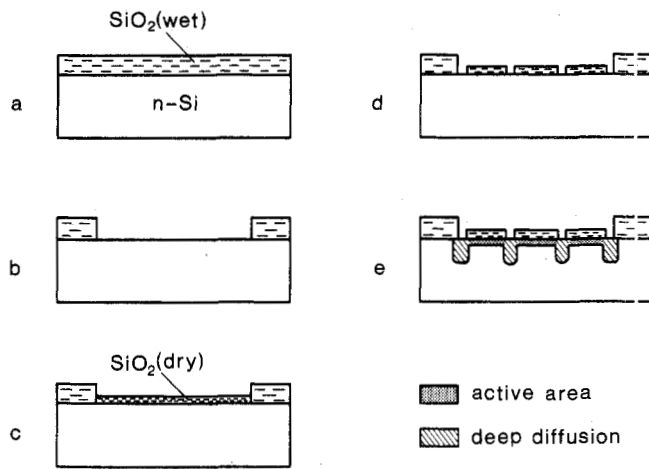


Fig. 2. Fabrication process for UV-sensitive photodiodes.

The process for generating UV-sensitive p-n diodes is shown in Fig. 2. The starting material is n-type silicon, Czochralski grown, (111)-oriented, with  $N_D = 10^{16} \text{ cm}^{-3}$ . A thick (3000 Å)  $\text{SiO}_2$  layer fixes the device limits (Fig. 2(a),(b)). A second (dry) oxidation process provides a thin (750 Å) oxide layer covering the surface of the device (Fig. 2(c)). As shown previously [7], a thin  $\text{SiO}_2$  layer can be used to control the surface acceptor concentration in silicon. Device regions with low and high surface concentrations (shallow and deep p-n junctions) can be produced simultaneously, if the thin oxide is removed selectively, as indicated in Fig. 2(d).

The diffusion process consists of a predeposition step and a drive-in step. The predeposition is performed in a sealed quartz tube with a powdered silicon/boron source ( $N_A = 2 \times 10^{20} \text{ cm}^{-3}$ ) at  $1000^\circ\text{C}$  for 1 h. The drive-in diffusion is carried out in a slightly oxidizing ambient at  $1150^\circ\text{C}$ . A diffusion process for a period of 8 h yields a boron surface concentration of  $2 \times 10^{16} \text{ cm}^{-3}$  and a junction depth of  $0.4 \mu\text{m}$  within the UV-sensitive area (which is covered by 750 Å  $\text{SiO}_2$ ). A guard ring and current paths with a surface concentration around  $2 \times 10^{19} \text{ cm}^{-3}$  are produced at the same time (Fig. 2(e)). The final step is a conventional aluminum metallization process. There are no gettering cycles involved, nor are any special precautions taken against contamination by lifetime-killing metal ions. The diodes have no anti-reflective coating, except for the 750-Å  $\text{SiO}_2$  layer which serves for the control of the boron surface concentration during the diffusion process.

Photodiodes with high UV sensitivity have been produced with active areas ranging from 0.14 to  $14 \text{ mm}^2$ . Fig. 3 shows the design of the largest diode type. The effects of various geometrical configurations and different junction depths will be discussed in the next section.

### III. SPECTRAL RESPONSE OF PHOTODIODES

The spectral response of boron-diffused photodiodes was measured by means of a deuterium lamp and a Jarrell-Ash Model 82-410 grating monochromator. Additional experiments were performed with reflection-type UV fil-

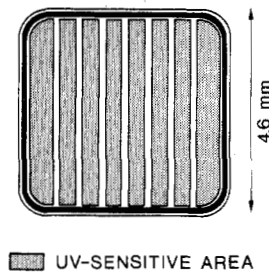


Fig. 3. Design (top view) of photodiode with  $14 \text{ mm}^2$  active area.

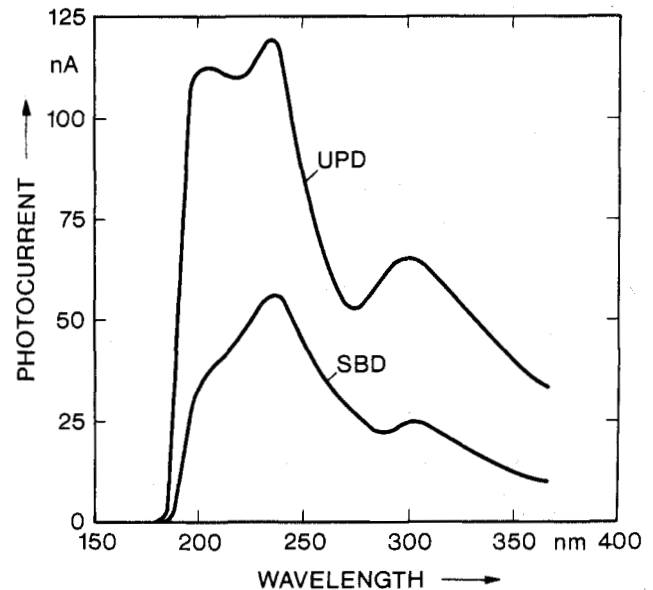


Fig. 4. Photocurrent generated in a UV photodiode (UPD) and in a Schottky-barrier detector (SBD); deuterium lamp.

ters (Schott) at 220, 250, 280, and 310 nm (15-nm half-width) and with interference filters at 312, 325, 338, 355, and 403 nm (7-nm half-width). Both types of measurement are in agreement within 5 percent. The incident light intensity was continuously monitored with a Schottky-barrier diode (United Detector Technology, Inc.) the calibration of which was checked with a bolometer-type radiation detector (Scientech, Inc., Model 360203) at the wavelengths available from the filters mentioned above.

In Fig. 4 a comparison is made between the photocurrent generated in the Schottky-barrier detector and in a UV-sensitive diode with a low boron surface concentration. The illuminated area is  $0.03 \text{ cm}^2$  in both cases. It can be seen from Fig. 4 that the boron-diffused UV diode gives a superior response to the deuterium lamp emission, especially in the 190- to 250-nm wavelength range.

The light source for measurements at wavelengths exceeding 400 nm was an incandescent lamp. The data obtained by means of the grating spectrometer were checked with interference filters (11-nm half-width).

Fig. 5 shows the responsivities of a diffused UV diode, a Schottky-barrier UV detector, and a commercial silicon solar cell (Siemens) in the 250- to 550-nm wavelength range. The incident light was restricted mainly to the UV-sensitive area. It is seen from Fig. 5 that the diffused

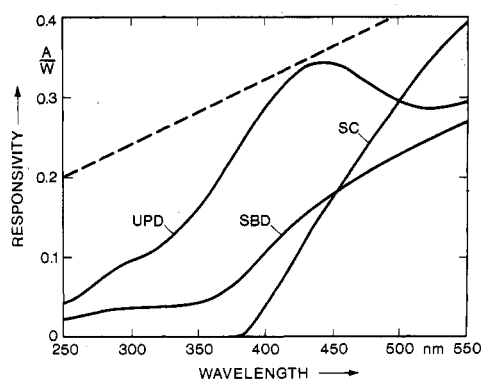


Fig. 5. Comparison of the responsivities of UV photodiode (UPD), Schottky-barrier UV detector (SBD), and conventional silicon solar cell (SC). Preferential illumination of UV-sensitive area. Dashed line: theoretical limit (100-percent quantum efficiency).

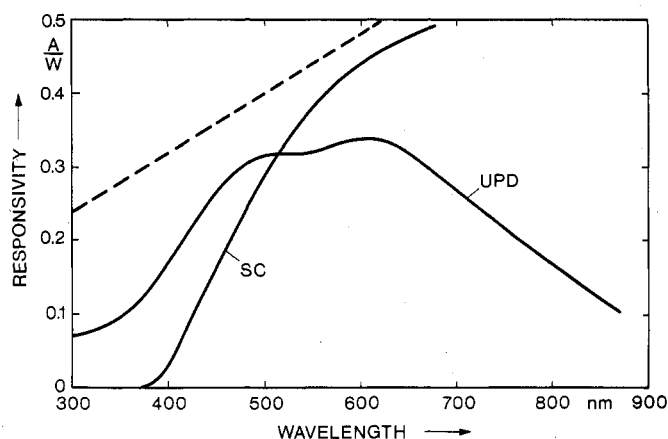


Fig. 6. Comparison of the responsivities of UV photodiode (UPD) and silicon solar cell (SC) with uniform illumination. Dashed line: theoretical limit (100-percent quantum efficiency).

diode exhibits a comparatively high responsivity in the UV and blue ranges of the spectrum. The peak responsivity (with nearly 100-percent quantum efficiency) is reached at 440 nm. The UV-enhanced diode is inferior to conventional solar cells beyond 500 nm.

The junction depth  $x_j$  below the UV-sensitive surface has to be adjusted to give optimum performance. About 600 devices have been produced with junction depths ranging from 0.1 to 2.3  $\mu\text{m}$ . It is found, in general, that the responsivity at 253 nm is close to 0.1 A/W for  $x_j < 0.2 \mu\text{m}$ . A nearly constant responsivity of 0.05 A/W is obtained with  $0.4 < x_j < 0.8 \mu\text{m}$ . A marked decrease of the UV sensitivity is observed for  $x_j > 1.3 \mu\text{m}$ . For a given junction depth, the spread of the UV sensitivities is less than  $\pm 5$  percent (50 devices).

A spectral response according to Fig. 6 is obtained when UV diodes with junction depths ranging from 0.4 to 0.8  $\mu\text{m}$  are illuminated uniformly (i.e., radiation incident on regions with shallow and deep p-n junctions, see Fig. 2(e)). The UV responsivity is slightly reduced in this case, whereas carriers collected within the deep p-regions contribute to the response around 600 nm. Thus a combined spectral response results which is quite flat from 450 to 650 nm. It is expected that the responsivity in the long-wave-

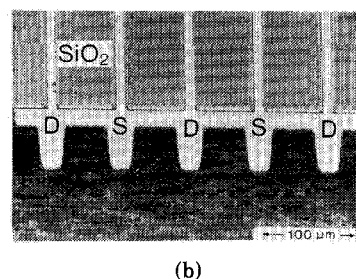
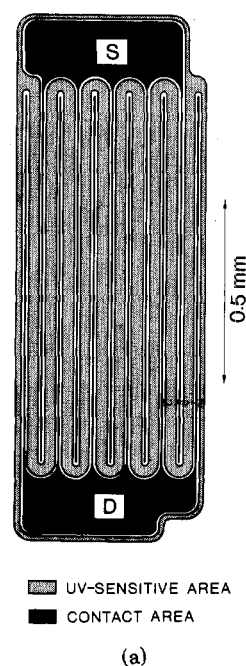


Fig. 7. (a) Basic design of large-area UV-sensitive field-effect transistors. (b) Angle-lap ( $1^\circ$ ) through field-effect transistors with 60- $\mu\text{m}$  nominal channel length.

length region can be enhanced by increasing the carrier lifetime with conventional gettering techniques.

Most optical (responsivity) data were taken at a radiation intensity around  $10 \mu\text{W}/\text{cm}^2$ . The response of the UV-sensitive diodes (and of the field-effect transistors operating in the diode mode) is linear in the flux range from  $0.1 \mu\text{W}/\text{cm}^2$  to  $100 \text{ mW}/\text{cm}^2$ , at least.

#### IV. PHOTOSENSITIVE JUNCTION FIELD-EFFECT TRANSISTORS

Photosensitive field-effect transistors have been produced with a basic design according to Fig. 7(a). The (n-type) bulk material serves as a gate. The diffusion parameters are similar to those described in Section II for UV diodes. Fig. 7(b) is a photomicrograph of an angle-lap through an FET device (before metallization). The regions with shallow diffusion depth are UV sensitive, whereas the deeply diffused areas constitute source and drain areas. The devices can be operated as diodes in the photovoltaic mode (source and drain short-circuited), in the photoconductive mode (gate and source short-circuited), or in the FET mode (with gate bias).

The dimensions and some technological data for three main types ("A," "B," and "C") of photosensitive FET's are listed in Table I. The channel lengths given in Table

**TABLE I**  
**Design and Technological Data of UV-Sensitive Field-Effect Transistors**  
**Responsivity in Photodiode Mode at 253 nm**

	FET type "A"	FET type "B"			FET type "C"
		1	2	3	
Nominal Channel length ( $\mu\text{m}$ )	60	40			30
Photosensitive area ( $\text{mm}^2$ )	0.81	0.37	0.31	0.37	0.37
Bulk donor concentration ( $\text{cm}^{-3}$ )	$4 \times 10^{15}$	$1.1 \times 10^{16}$			$6 \times 10^{15}$
Junction depth ( $\mu\text{m}$ )	0.8	0.1	0.27	0.84	0.1
Sheet resistivity ( $\Omega$ )	36 k	520 k	82 k	17 k	580 k
Boron surface concentration ( $\text{cm}^{-3}$ )	$7.5 \times 10^{15}$	$1.4 \times 10^{16}$	$2 \times 10^{16}$	$3 \times 10^{16}$	$8.5 \times 10^{15}$
Responsivity at 253 nm (A/W)	0.11	0.067	0.065	0.065	0.10

I correspond to the dimensions of the oxide pattern; a certain amount of lateral diffusion (in the order of 5–10  $\mu\text{m}$ ) has to be taken into consideration in calculating the actual (UV-sensitive) lengths. It can be seen from Table I that the highest responsivity in the diode mode at 253 nm was obtained with a low bulk donor concentration and a boron surface concentration adjusted accordingly (types "A" and "C"). The channel length is not critical for the operation in the diode mode.

The electrical properties of the field-effect transistors are, of course, dependent on the channel size and the doping level. Usually, the pinchoff voltage of the devices described in this paper is in the 0.8- to 3-V range. The responsivity data given in Table I are extracted from measurements performed with 50 devices per wafer, approximately.

The speed of response was tested with modulated laser beams. The photovoltaic decay time decreases with decreasing wavelength from 250 ns at 660 nm to 40 ns at 337 nm (100- $\Omega$  load resistance). A further reduction of the decay time (by a factor of four) is obtained with a reverse bias of 20 V. These data were taken from FET devices with design "A" operated as diodes.

Fig. 8 is a comparison of the responsivities when operating a device of type "C" in the photovoltaic mode, the photoconductive mode, and the FET mode. The device exhibits a nonlinear characteristic with a saturation current of 150  $\mu\text{A}$  for  $0.3 \leq V_{DS} \leq 5$  V if the source and gate contacts are short-circuited ( $V_{GS} = 0$ ). The drain current drastically increases when the device is illuminated. As seen from Fig. 8, a responsivity around  $10^3$  A/W can be obtained for the UV region. This means that operation in the photoconductive mode yields a gain in the order of  $10^4$  for short-wavelength radiation; the high gain is due to UV photon absorption in the very shallow ( $x_j \approx 0.1$   $\mu\text{m}$ ) p-type channel. The gain decreases monotonically with increasing wavelength, since low-energy photons are producing free carriers mainly within the bulk material; these carriers do not contribute to the conductivity modulation of the channel.

The standing current can be considerably reduced if the gate is appropriately biased (FET-mode). The gain in the UV region is lower by an order of magnitude, approxi-

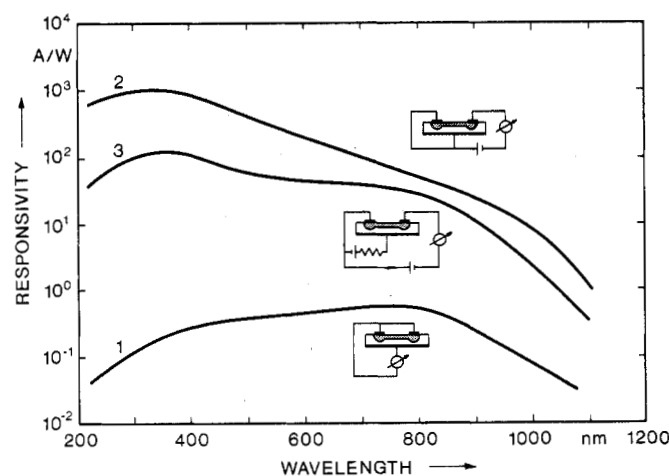


Fig. 8. Responsivity versus wavelength of FET (design "C"). Curve 1: operation in photovoltaic (diode) mode (UV intensity varying from 10 to 100  $\mu\text{W}/\text{cm}^2$ ). Curve 2: operation in photoconductive mode (UV intensity 15  $\mu\text{W}/\text{cm}^2$ ). Curve 3: operation in FET mode ( $V_{GS} = 0.6$  V,  $R_G = 1$  M $\Omega$ , 150  $\mu\text{W}/\text{cm}^2$ ).

mately, with the operating conditions shown in Fig. 8 (dark current 1  $\mu\text{A}$ ,  $V_{GS} = 0.6$  V). This is due to space-charge widening in the channel region (i.e., reduction of the effective channel thickness). The responsivity decreases drastically when the transistor is biased beyond pinchoff ( $>0.8$  V for type "C" devices).

If a resistor is inserted into the gate circuit, a contribution to the gate voltage generated by the photocurrent is noticed. The shift of the gate voltage yields an additional amplification mechanism, which is effective mainly for the medium-wavelength radiation, i.e., for those photons which give maximum responsivity in the photovoltaic mode. Thus the spectral response curve can be adjusted for a specific application by proper choice of the operating conditions.

The response of the UV-sensitive devices operated in the photoconductive and FET modes is nonlinear at high radiation flux levels (decreasing sensitivity with increasing light intensity).

## V. APPLICATIONS OF UV-SENSITIVE DEVICES

A new field of applications is opened by the extension of the responsivity of silicon photodiodes and photosen-

sitive FET structures into the UV to 190-nm wavelength and lower. This extension not only permits measuring UV light with relatively simple silicon devices but also makes available elements of remarkably broad banded responsivity (190–1100 nm). The diodes show good linearity over many decades of irradiance. They yield low values of noise equivalent power (NEP) and are especially suited for low-level light detection (e.g.,  $10^{-12}$  W) and for the detection of fast laser pulses.

In recent years a number of lasers have been developed which operate at blue or UV wavelengths (e.g., nitrogen laser at 337 nm, He–Cd laser at 325 nm). These lasers are about to enter fields such as absorption spectroscopy, resonance fluorescence, photoionization, pollution detection, and others. Dye lasers are of particular value in these applications due to their tunability [8]. The radiation emitted by these lasers can be detected by the diodes and FET's described above.

UV-sensitive detectors are useful also for applications employing radiometric or colorimetric measurements. In particular, colorimetry is often used for the quantitative determination of chemical or biochemical reaction products. In this way, for example, proteins can be determined

at 280 nm and nucleic acid at 260 nm. Many enzymatic reactions where pyridine nucleotides are involved usually require a measurement at 334 nm. The detectors are further useful for measuring UV intensities at 253 nm (principal emission of mercury lamps). UV light of this wavelength is used for air sterilization in hospitals and laboratories, in food processing, and similar applications.

#### REFERENCES

- [1] J. Lindmayer and J. F. Allison, "The violet cell: An improved silicon solar cell," *COMSAT Tech. Rev.*, vol. 3, pp. 1–22, 1973.
- [2] R. F. McQuat and D. C. Pulfrey, "Analysis of silicon Schottky barrier solar cells," in *Conference Record of the 11th Photovoltaic Specialists Conference*, 1975, pp. 371–375.
- [3] G. C. Salter and R. E. Thomas, "Induced junction silicon solar cells," in *Conference Record of the 11th Photovoltaic Specialists Conference*, pp. 364–370, 1975.
- [4] L. Forbes and J. R. Yeargan, "Design for silicon infrared sensing MOSFET," *IEEE Trans. Electron Devices*, vol. ED-21, pp. 459–462, Aug. 1974.
- [5] W. C. Parker and L. Forbes, "Experimental characterization of gold-doped infrared sensing MOSFET's," *IEEE Trans. Electron Devices*, vol. ED-22, pp. 916–924, Oct. 1975.
- [6] A. S. Grove, *Physics and Technology of Semiconductor Devices*. New York: Wiley, 1967.
- [7] W. v. Muench and C. Gessert, "Low surface concentration of boron in silicon by diffusion through silicon dioxide," *J. Electrochem. Soc.*, vol. 122, pp. 1685–1689, 1975.
- [8] F. P. Schaefer, "Dye lasers," in *Topics in Applied Physics*, vol. 1, Berlin: Springer, 1973.